encit 2020

ABCM Associação Brasileira de Engenharia e Ciências Mecânicas

18th Brazilian Congress of Thermal Sciences and Engineering
November 16–20, 2020 (Online)

ENC-2020-0174
DEVELOPMENT OF A BALLISTIC EVALUATION MOTOR FOR KNSU BURN RATE MEASUREMENTS

Carlos Eduardo Américo
Laboratory of Numerical Experimentation (LENA), Department of Mechanical Engineering (DEMEC), Universidade Federal do Paraná (UFPR), Caixa postal 19040, Zip Code 81531-980, Curitiba, Paraná, Brazil.
ceamerico123@hotmail.com

Diego Fernando Moro
Positivo University (UP), Department of Mechanical Engineering, Zip Code: 81280-330, 5300 Professor Pedro Viriato Parigot de Souza Street, Curitiba, PR, Brazil.
diego.moro@up.edu.br

Carlos Henrique Marchi
Federal University of Paraná (UFPR), Department of Mechanical Engineering (DEMEC), Zip Code: 81531-980, Caixa postal 19040, Curitiba, PR, Brazil.
chmcfd@gmail.com

Filipe Melo de Aguiar
Laboratory of Numerical Experimentation (LENA), Department of Mechanical Engineering (DEMEC), Universidade Federal do Paraná (UFPR), Caixa postal 19040, Zip Code 81531-980, Curitiba, Paraná, Brazil.
filipemelo111@gmail.com

Abstract. *In this work, the burning rate of KNSu propellant, understood as a mixture of Potassium Nitrate and Sucrose cold pressed, is estimated analytically by results from Ballistic Evaluation Motor (BEM) experimental tests. The BEM can provide an experimental approach related to the pressure inside the combustion chamber and also, provide analysis related to expansion of gases and thrust generation by nozzles interchangeability. Those experiments were realized via static tests focusing in the instantaneous burning rate versus the absolute pressure (obtained by analogical instrumentation and digital software) and estimated pressure (obtained by numerical estimation). Furthermore, five different nozzles were employed and had their specific impulse, total impulse and thrust calculated for each of them. The results show that KSNu propellant, cold pressed, has an exponential tendency between instantaneous burning rate and chamber pressure. Also, for low pressures applied on this work, the divergent section do not contributed significantly to average thrust value.*

Keywords: *experimental rocket, burning rate, thrust, KNSu, specific impulse.*

1. INTRODUCTION

Among all kinds of data that can be obtained experimentally by a Ballistic Evaluation Motor (BEM), there is one especial property interpreted as burn velocity versus time, also known as burning rate. This property is related to the chamber pressure and temperature during the steady state burning grain (the rigid mass of propellant with specific form, geometry and burning area). Research concerning burning grains can be obtained by experimental tests, using a Crawford pump (with this equipment, the combustion pressure is previously fixed) or one Ballistic Evaluation Motor by applying analytical relations between the pressure curve and propellant burning time, Nakka (2003).

Understanding how quickly the burning process occurs inside the combustion chamber is one requirement needed for predicting the force generated by an experimental rocket, in other words, thrust. Motivated by this statement, the main objective of this work was to design, fabricate and test one BEM for burning properties evaluations of the KNSu propellant, assessing the pressure inside the burning chamber and its relation to the instantaneous burn rate. This relation is calculated following the method described by Nakka (2001a). Another possible analysis is the relation between different nozzles and thrust generation, once the convergent section of the internal geometry remains unchanged for all nozzles and the divergent section of each one is slightly different from the others, changing length and half divergent angle. The Fig. 1 illustrates all parts that compose the BEM assembled, named in this work as MTPβ. Each test is named by this acronym and one additional number. Since nine tests were made, the experiment names are labeled from MTPβ-1 to MTPβ-9.

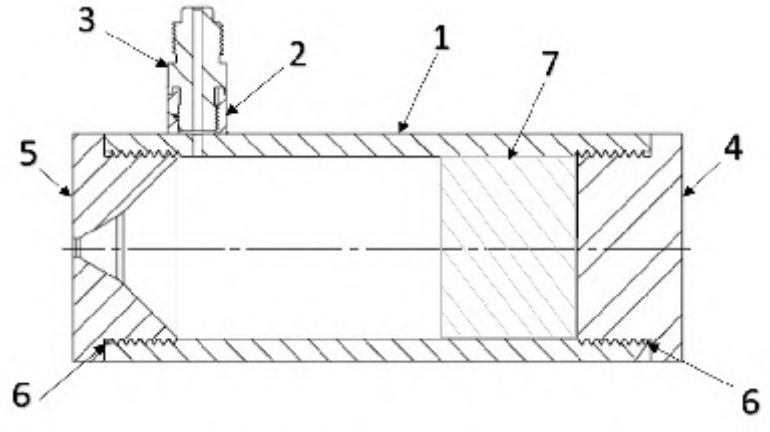

Figure 1. Ballistic Evaluation Motor scheme.

The numbered items can be described as:

- 1 - Main tube: responsible for components assemble and structural resistance. The region inside this component is named combustion chamber.
- 2 - Welded connector: links the main tube surface with the pressure plug.
- 3 - Pressure plug: links the internal pressure with the pressure gauge.
- 4 - Screw cap: close and seal the combustion chamber.
- 5 - Nozzle: responsible for accelerating the generated gases and generate thrust.
- 6 - Seal rings: its deformation when the nozzle and screw cap are attached prevents pressure and gas leak.
- 7 - Propellant: flammable mixture between oxidant and fuel.

Moreover, Miller (1971) recommends that: burning rate evaluation should be made in one specific type of propellant grain, named end-burner (solid cylinder block of propellant where the cross section is the only ignited region); propellant grain length must be minor than two times the cross section diameter; the propellant burning face area must have at least six times the throat area; the burning time should not exceed ten seconds. All those suggestions were followed during planning and BEM design.

2. LITERATURE REVIEW

Before proceeding to main objective of this work, there is some definitions and physical concepts that must be presented first. Firstly concept to be introduced is propellant. It can be understood as the product of a mixture between oxidant and fuel, mixed at some proportion. Sutton and Biblarz (2008) describe that the propellant and its geometry is directly responsible for the thrust generated. Nakka (2001b) recommends that some requirements should be evaluated before selecting the most appropriate propellant, some of them are: handle and storage security; toxicity of each component; fumes; burning predictability and its manufacture procedures.

Some propellants can be mentioned, for example: Mixture between Potassium Nitrate and Sucrose (KNSu); Potassium Nitrate and Sorbitol (KNSB) and Potassium Nitrate and Dextrose (KNDX). In this work, the propellant KNSu was selected because it agrees really well with the previously recommendations and components availability. Although must be said that each component is not completely pure, since the mixture of Potassium Nitrate comes from Krista K™fertilizer and it has two percent of Magnesium and Sulfur. Same situation for sucrose, since the source for it comes from refined white sugar, which is not completely pure. Foltran *et al.* (2014) calculate an approximation for the experimental KNSu density, considering the absence of porosity and the lack of purity, by applying the Eq. 1.

$$\rho_t = \frac{1}{\frac{x_{su}}{\rho_{su}} + \frac{x_{kn}}{\rho_{kn}}} \cong 1888 \frac{kg}{m^3} \tag{1}$$

where ρ_{kn} and ρ_{su} is the Potassium Nitrate and Sucrose density, (2109 kg/m^3) and (1581 kg/m^3) respectively; x_{kn} and x_{su} are the mass fraction of Potassium Nitrate and Sucrose, equal to 0.65 and 0.35, respectively.

Another important property is burn rate. Miller (1971) affirms that independently of the propellant, it can be calculated by an empirical relation:

$$r = ap_0^b \tag{2}$$

where r represents the burning rate; p_0 is the stagnation pressure inside the combustion chamber; a is an experimental pressure coefficient and b is the burning rate exponent, also found experimentally. This relation is called Saint Robert's Law and is valid only for low values of mass flow and was shown on its simplified version. Additional details about the Eq. 2 can be found in Miller (1971).

One of the most important properties measured by this test is thrust (F). As said by Humble *et al.* (1995), thrust comes from the second Newton's law, where the summation of applied external forces is equal to the variation of momentum. This concept formulated for nozzles can be expressed as:

$$F = p_0 A_t \sqrt{\left(\frac{2}{\gamma+1}\right)^{\frac{\gamma+1}{\gamma-1}} \frac{2\gamma^2}{\gamma-1}\left[1-\left(\frac{p_e}{p_0}\right)^{\frac{\gamma-1}{\gamma}}\right]} + (p_e - p_a)\, A_e \tag{3}$$

where γ is the specific heat ratio; A_t is the nozzle throat area; A_e is the exit nozzle area; p_a and p_e are atmospheric pressure and exhaust pressure, immediately after the nozzle exit, respectively.

Also, two efficiency parameters were evaluated. The first one is the specific impulse I_s. Understood as the quantity of impulse generated by the amount of propellant. Its value is directly proportional to the quality of the entire propulsion system and can be calculated as:

$$I_s = \frac{\int_0^t F dt}{g m_p} \tag{4}$$

where g is gravitational acceleration; m_p is the propellant mass; F is thrust and t is the burning time.

The second efficiency parameter is the thrust coefficient. Sutton and Biblarz (2008) said that the objective of this parameter is to evaluate the nozzle efficiency, by an algebraic relation between thrust, stagnation pressure and nozzle throat area. This coefficient is calculated by:

$$C_f = \frac{F}{p_0 A_t} \tag{5}$$

3. NOZZLES GEOMETRY

Nozzle, basically, is the equipment responsible for accelerating the generated gases, as result of this acceleration, thrust is generated. The convergent half angle was selected based on Germer (2014). In this work, the author compares various opening angles and, theoretically, the 30 degrees was the one which had the better thrust coefficient.

All nozzles used in this work are present in Fig. 2. The internal geometry is divided in two sections, the convergent (black contour) and divergent section. Each of them received a identification dependent of each divergent section, since all of them had the same convergent, the different nozzles are named based on divergent geometry.

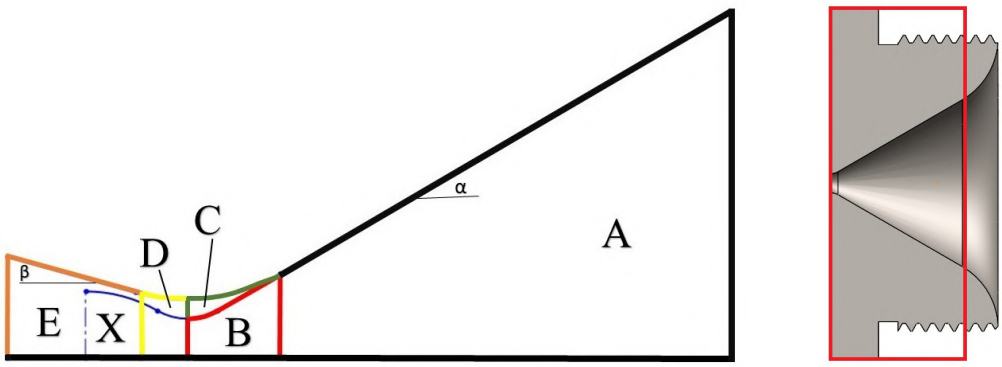

Figure 2. Internal nozzle profile.

Table 1 shows geometrical data for all tested nozzles. Where Dg_r is the nozzle throat; Dc is the convergent diameter; Dd is the divergent diameter; α is the convergent half angle measured in degrees and β is the divergent half angle, also measured in degrees. Nozzle "B" and "C" do not have a divergent section.

Table 1. Nozzles geometric data.

Nozzle	$Dg_r\ (mm)$	$Dc\ (mm)$	$Dd\ (mm)$	α	β
B	4.24	34.94	-	30.00 ± 1	-
C	6.08	36.10	-	28.45 ± 1	-
D	5.93	35.16	6.79	30.25 ± 1	9.50 ± 1
X	4.18	34.22	6.77	30.15 ± 1	15.00 ± 1
E	5.96	36.19	10.32	32.75 ± 1	17.16 ± 1

4. EXPERIMENTAL APPROACH

The first step is the propellant manufacturing. Initially, both Potassium Nitrate and Sucrose are individually ground by rotating blades. Subsequently, they are mixed at 0.65/0.35 weight proportion (Potassium Nitrate and Sucrose, respectively) and dumped inside the combustion chamber. The propellant grain are molded by mechanical compression via mechanical press, gradually increasing the applied force until reaching and stabilizing at 10 ton. After this procedure, the propellant grain is measured and the static test can be done.

4.1 Static Test

The experimental rocket was horizontally positioned on a static bench equipped with a load cell and manometers, as shown in Fig. 3.

Figure 3. Complete assemble with digital and analogical instrumentation.

The generated thrust is turned to electrical signal by the load cell deformation (type S2; made by Hottinger Baldwin Messtechnick GmbH - HBM; maximum force accepted equal to 200 N; resolution equal to 0.025 N; 200 Hz sample frequency, meaning 0.005 s between each measurement), then the signal goes to the acquisition data module Spider 8 (HBM) and communicates with the software Catman 4.5. The manometers were manufactured by Tecno™.

After the data acquisition for thrust and time, the results are sent to a software called Curva_Empuxo3p2, and with it was calculated: medium thrust; burning time; specific impulse; total impulse; maximum and minimum forces;average exhaust velocity and estimated pressure (applied for instantaneous burning rate calculation). This software is described and provided by GFCS (2018).

4.2 Absolute pressure curves

The absolute pressure evaluation begins with local atmospheric pressure measurement for every static test (since the absolute pressure value is the summation between atmospheric pressure and manometric pressure). During the experimental rocket engine operation the pressure gauge indicator was recorded by film. The resulting files were sent to the software "Tracker Video Analysis and Modeling Tool for Physics Education", available in OSP (2018). Based on points distribution along the indicator, the pressure curve were obtained for each recorded frame. Additionally, some hysteresis may be present and some frames couldn't be accurately estimated by Tracker, so for this reason, when this type of problem occurred, the average pressure between to accurate estimated frames were applied. Finally, the local pressure was added to manometric pressure to obtain the absolute pressure, and with it calculate the instantaneous burning rate measured.

5. NUMERICAL APPROACH

The instantaneous burn rate evaluation based on absolute pressure measurements are based on Nakka (2001a) and its value is calculated by:

$$\Delta_s(t) - \frac{A_t}{A_b(s(t))}\frac{p_0(t)}{\rho c}\Delta_t = 0 \tag{6}$$

where Δ_t is the time step at each thrust measurement, equal to $0.005s$; c is the exhaust fluid velocity; $\Delta_s(t)$ is the face burning regression at each time step measured as length; $s(t)$ is the surface regression, equal to $\Delta_s(t)$ plus one initial value, understood as an correction value to fit the final total burning face regression with total grain length; $A_b(s(t))$ is the burning face area at each time step. Since the propellant grain has only one burning surface, limited by the cross section, this variable has a constant value and $p_0(t)$ is the stagnation pressure measured at each time step. The instantaneous burning area is equal to $\Delta_s(t)$ divided by Δ_t.

6. RESULTS

As multiple nozzles were applied on this work (consequently different exhaustion areas), Tab. 2 brings propellant grain length (L_g), atmospheric temperature (T_a), atmospheric pressure (P_a), nozzle and date for each test. Also, for sake of brevity, absolute pressure was abbreviated by AP; estimated pressure was abbreviated by EP and instantaneous burning rate, IBR. Additionally, Tab. 2 shows the average values of IBR calculated with AP and EP for each test using Eq. 6, named $aIBR_{AP}$ and $aIBR_{EP}$, respectively.

Table 2. Test name, propellant grain length, nozzles, dates, atmospheric properties and IBR values for each test.

Test	Lg (mm)	$T_a(^\circ C)$	$P_a(hPa)$	Nozzle	Date	$aIBR_{AP}(mm/s)$	$aIBR_{EP}(mm/s)$
MTPβ-1	24	20.4	910.6	B	02/09/18	12.61788	-
MTPβ-2	24	19.2	911.1	B	02/09/18	9.37101	8.78311
MTPβ-3	25	19.0	911.2	X	02/09/18	-	15.30969
MTPβ-4	27	15.6	908.1	C	16/09/18	6.90979	7.02968
MTPβ-5	27	16.1	908.0	E	16/09/18	5.42451	5.15759
MTPβ-6	26	17.3	907.2	D	16/09/18	5.52783	5.85984
MTPβ-7	27	19.7	906.5	C	30/09/18	10.74856	4.29895
MTPβ-8	28	20.2	906.6	D	30/09/18	5.86285	7.15961
MTPβ-9	29	21.0	906.2	E	30/09/18	-	6.44484

Table 3 shows the average thrust (Em), burning time (tq), average specific impulse (Iem), total impulse (It), average estimated pressure ($PavgE$), maximum average pressure ($PmaxE$), maximum thrust (Frm) and average thrust coefficient (Cf_{avg}) obtained by Curva_Empuxo3p2 and Catman 4p5.

Table 3. Results obtained by Curva_Empuxo3p2 and Catman 4p5.

Test	$Em(N)$	$tq(s)$	$PmavgE(bar)$	$PmaxE(bar)$	$Frm(N)$	Cf_{avg}	$Iem(s)$	$It(Ns)$
MTPβ-2	16.50	3.98	12.40	21.70	29.50	0.925	66.90	65.60
MTPβ-3	68.20	1.40	49.80	319.00	440.00	0.989	97.30	95.40
MTPβ-4	8.85	6.03	3.47	5.52	15.60	0.736	55.00	53.40
MTPβ-5	9.07	5.10	3.64	4.86	12.90	0.845	48.60	46.30
MTPβ-6	8.79	4.80	3.57	4.82	12.70	0.831	44.30	42.20
MTPβ-7	9.93	5.75	3.79	5.63	16.00	0.786	57.60	57.00
MTPβ-8	9.94	5.40	3.95	5.20	13.90	0.844	56.10	54.40
MTPβ-9	9.64	5.59	3.83	6.01	16.60	0.797	56.10	53.90

Once three different days were necessary to perform the experimental evaluations, distinct values for atmospheric temperature can be noticed (thermal equilibrium between the propellant grain and atmospheric temperature before grain ignition is assumed). Comparing maximum thrust values for tests with the same nozzle, for instance: MTPβ-4 with MTPβ-7; MTPβ-6 with MTPβ-8 and MTPβ-5 with MTPβ-9, there is an increase in temperature indeed (4.1 °C; 2.9 °C and 4.9 °C, respectively), but not strong enough to be directly related to thrust/pressure increase.

The first test, MTPβ-1, was made without digital measurements, because the main objective of this test was to ensure structural integrity and resistance. The only experimental data obtained from MTPβ-1 was the pressure inside the combustion chamber, measured with the pressure gauge and with it, instantaneous burning rate were calculated. Both absolute pressure and instantaneous burning rate are present in Fig. 4.

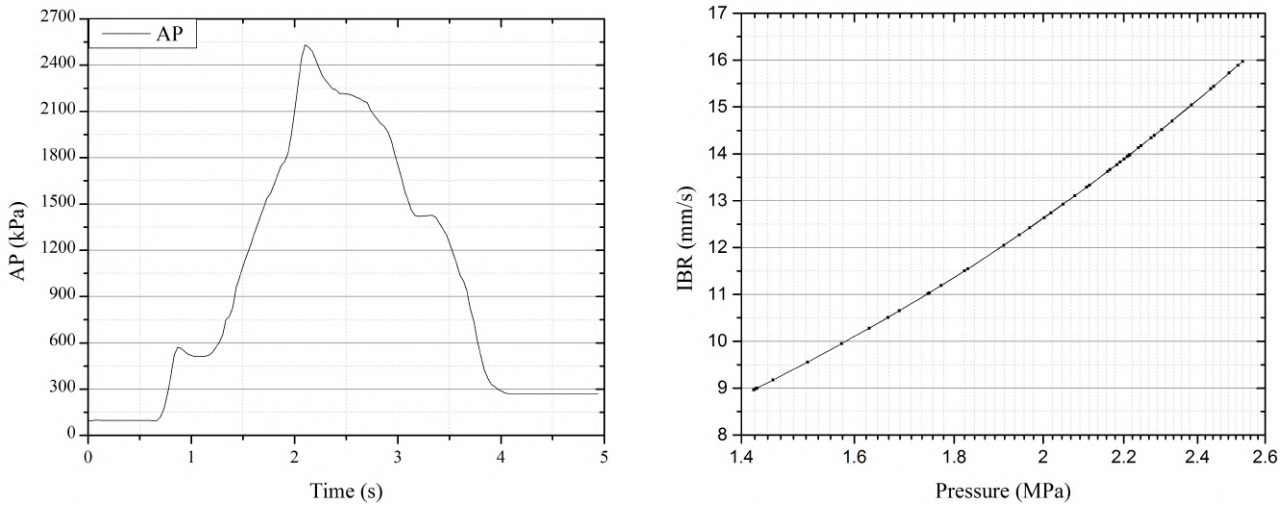

Figure 4. Absolute pressure versus time and instantaneous burning rate versus absolute pressure for MTPβ-1 test.

Since MTPβ-1 test was successful, the same assembly was tested again, but now with complete instrumentation, named MTPβ-2. Results for Thrust, estimated pressure, absolute pressure and instantaneous burning rate are shown in Fig. 5.

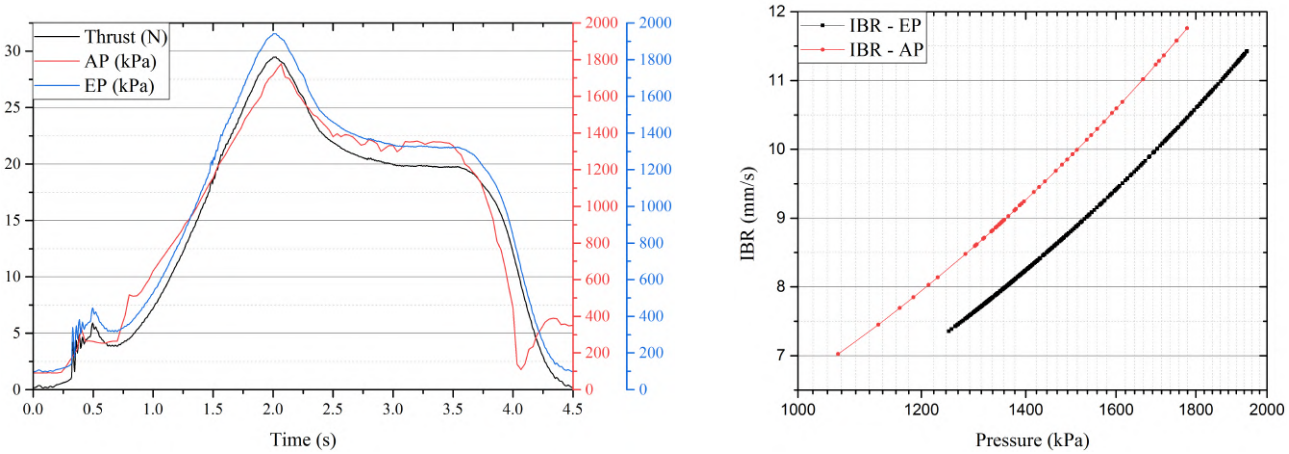

Figure 5. Thrust, absolute pressure, estimated pressure versus time and instantaneous burning rate versus chamber pressure for MTPβ-2 test.

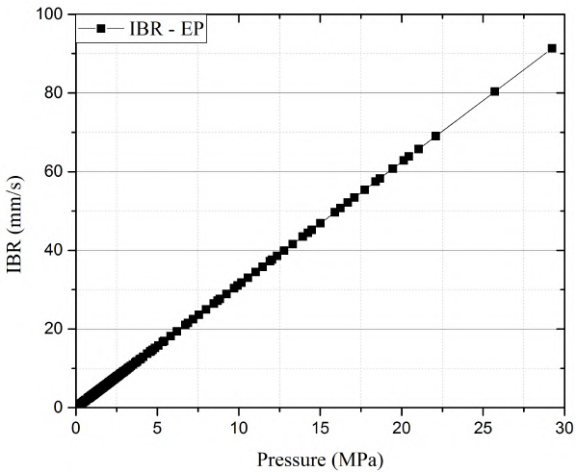

Figure 6. Instantaneous burning rate versus estimated pressure for MTPβ-3 test.

Thrust curve, estimated pressure, absolute pressure and instantaneous burning rate for MTPβ-4 until MTPβ-9 test are shown in Fig. 7 to Fig. 12.

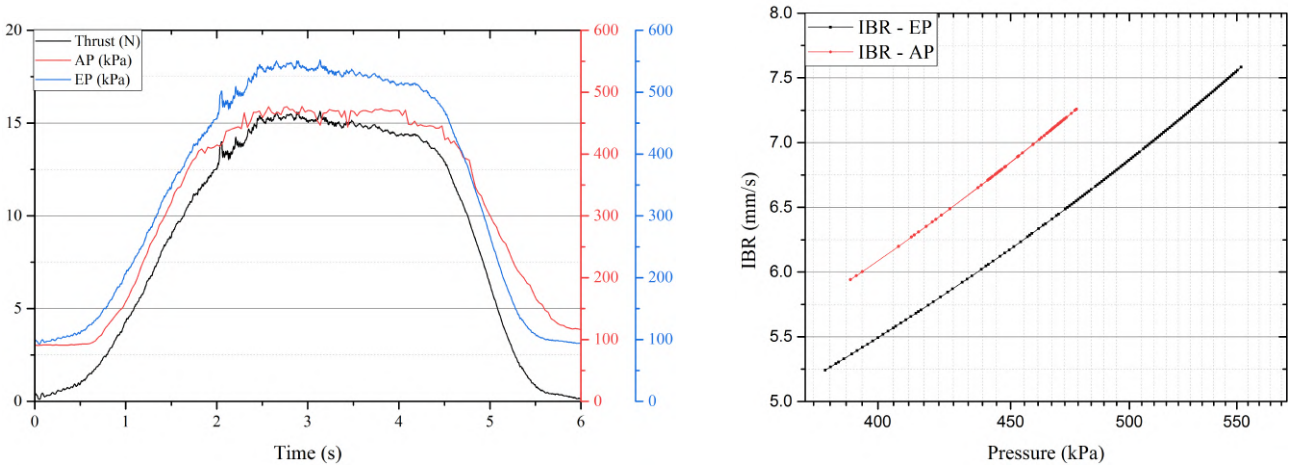

Figure 7. Thrust, absolute pressure, estimated pressure versus time and instantaneous burning rate versus chamber pressure for MTPβ-4 test.

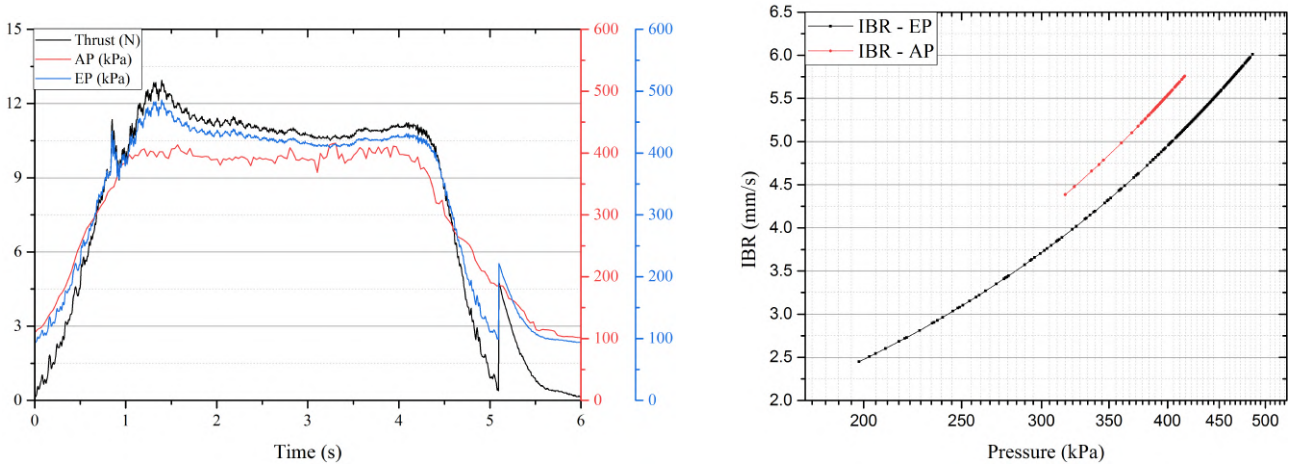

Figure 8. Thrust, absolute pressure, estimated pressure versus time and instantaneous burning rate versus chamber pressure for MTPβ-5 test.

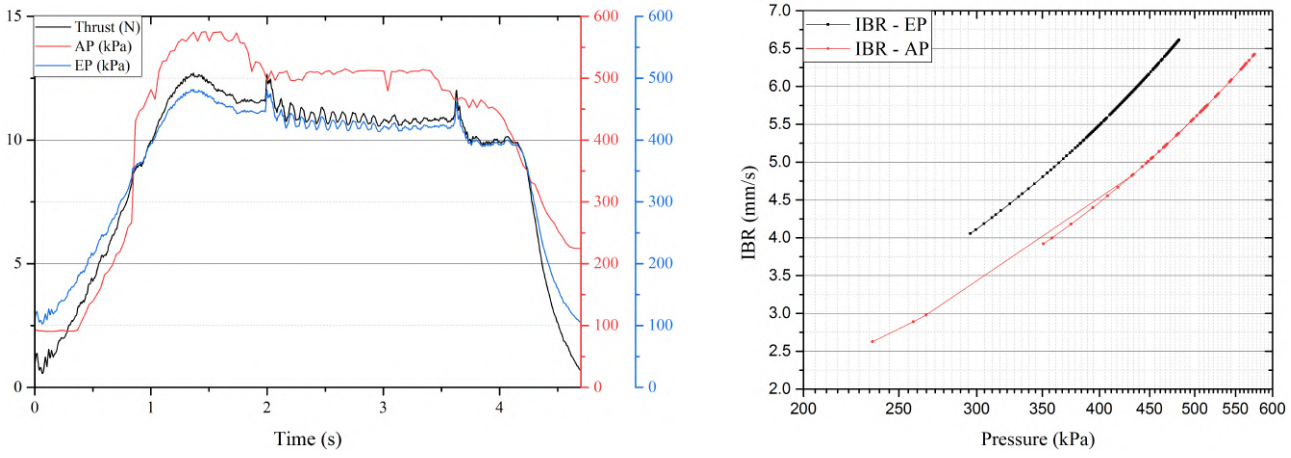

Figure 9. Thrust, absolute pressure, estimated pressure versus time and instantaneous burning rate versus chamber pressure for MTPβ-6 test.

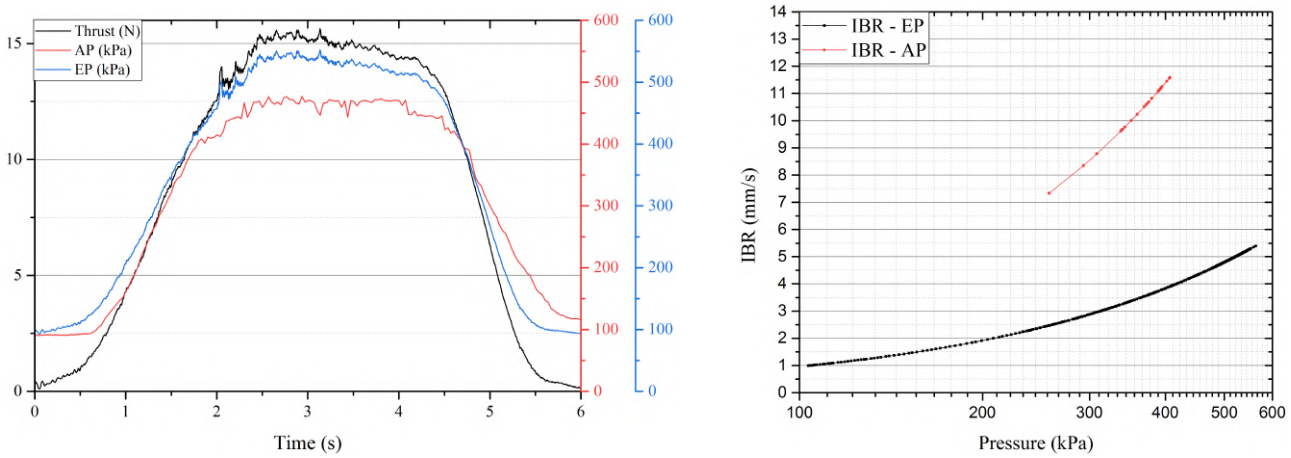

Figure 10. Thrust, absolute pressure, estimated pressure versus time and instantaneous burning rate versus chamber pressure for MTPβ-7 test.

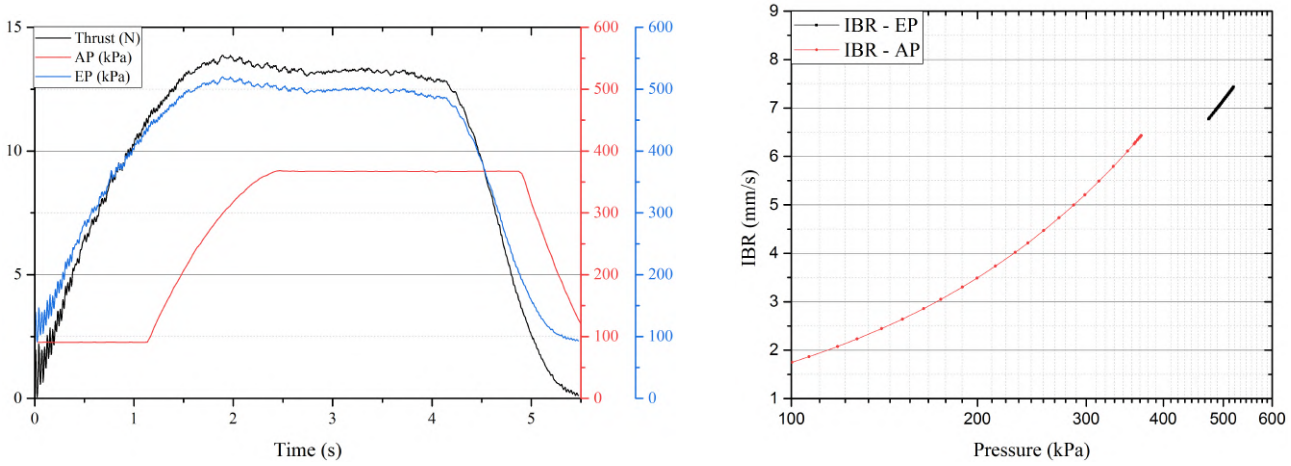

Figure 11. Thrust, absolute pressure, estimated pressure versus time and instantaneous burning rate versus chamber pressure for MTPβ-8 test.

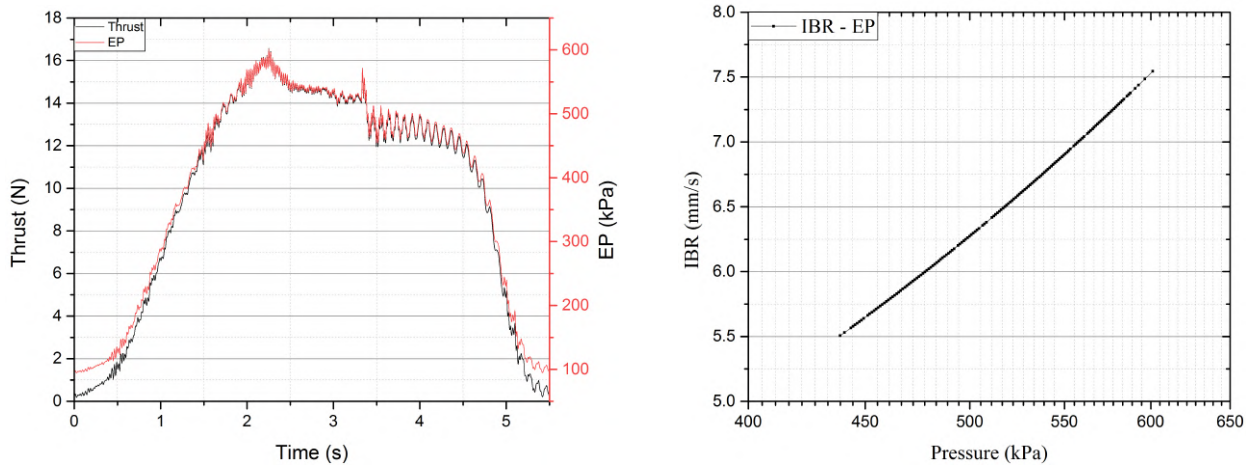

Figure 12. Thrust, absolute pressure, estimated pressure versus time and instantaneous burning rate versus chamber pressure for MTPβ-9 test.

Figure 6 shows only one graph, the instantaneous burning rate for the estimated pressure for MTPβ-3 test. This happened because the combustion chamber over pressurized and due it, the manometer collapsed and its measures or even the pointers footage couldn't be considered valid.

Figure 13 and Fig. 14 shows one global comparative between instantaneous burning rate calculated with estimated and absolute pressure for all valid tests (except for MTPβ-3 test). Additionally, two Saint Robert's curves were fit that represents reasonably well the average values for burning rate at each graph, as well present in Tab. 2. For Saint Robert's curve obtained with absolute pressure a and n were 0.012 and 0.475, respectively. For the Saint Robert's curve obtained with estimated pressure a and n were 0.018 and 0.44, respectively. Likewise, were added the instantaneous burning rate calculated by Nakka (1999) for KNSu, KNSB and KNDX.

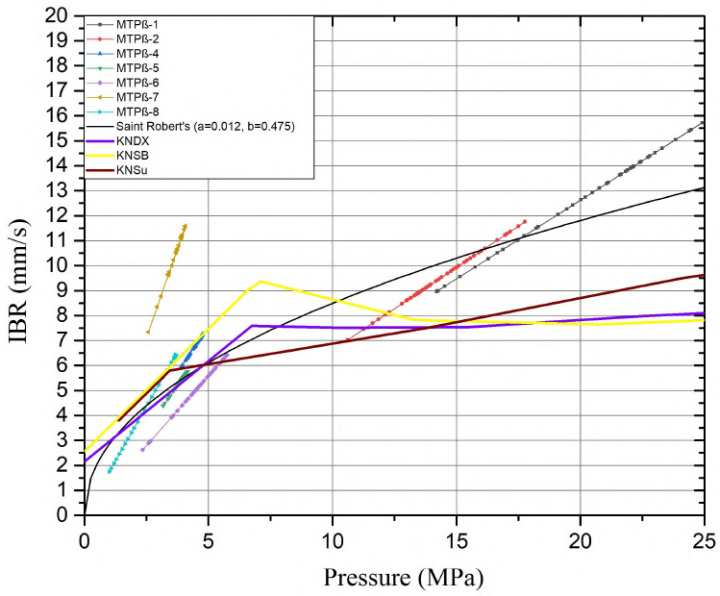

Figure 13. Instantaneous burning rate versus absolute pressure, Saint Robert's Law and Nakka (1999) results for KNSu, KNSB e KNDX.

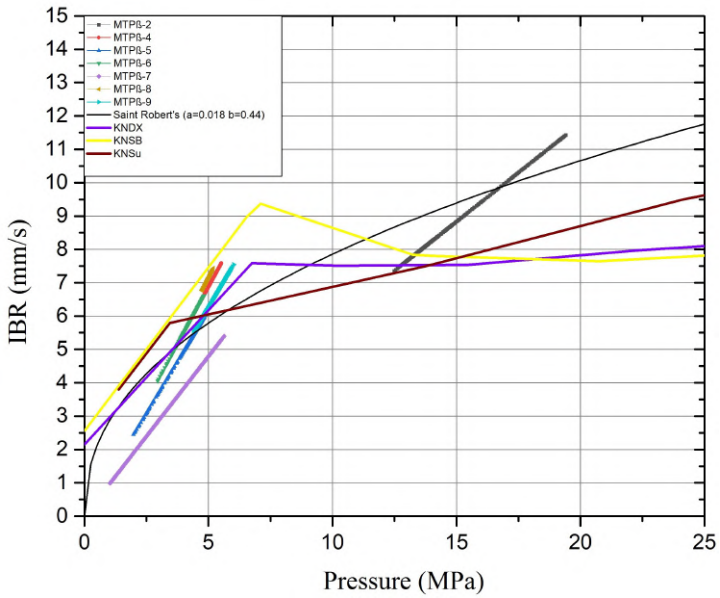

Figure 14. Instantaneous burning rate versus estimated pressure, Saint Robert's Law and Nakka (1999) results for KNSu, KNSB e KNDX.

Related to burning rate increase, Sutton and Biblarz (2008) describe one particular phenomenon known as burning enhancement by erosion (erosive burning), caused by the iteration between high speed combustion gases with the burning grain surface area. Usually, this enhanced burning rate occurs in the earlier burning phase and in hollow shaped propellant grains, initially increasing mass flow, heat transfer, pressure and thrust, leading to premature burning time. Apparently, this phenomenon also occurs in MTPβ-1 (due pressure peak around two seconds, and the absence pressure plateau) and MTPβ-2 (due thrust and pressure peak around two seconds).

Additionally, some combustion instability can be observed via irregularities in thrust and pressure curves for MTPβ-6

until MTPβ-9, once those curves shown oscillatory conditions. As said by Sutton and Biblarz (2008) acoustic instabilities (acoustic resonances or pressure oscillations) can occur with any rocket motor. Special attention must be addressed for MTPβ-6 estimated pressure/thrust curve, where small oscillations evolve for peaks, followed by more spaced oscillations until reach another peak. Curiously, this same pattern is described by the same authors in one of their figures in the textbook. This behavior leads to a rise in the mean pressure/thrust and reduction in the effective burning time.

7. CONCLUSION

The main results of this work can be summarized as follows:

- The average values of burn rate curves represents reasonably well the Saint Robert's curve for the evaluated pressure range. When those values are compared with the burn rate found by Nakka (1999), a different tendency is noted. The authors suspect that this happens because the confection process related to both propellant grains are different, although both have the same oxidant and fuel mixture rate, disregarding the purity of each component. Also, they are different when compared with KNDX and KNSB, but this last difference occurs because both KNDX and KNSB have non-linear burning characteristics.
- Results for average specific impulse and average thrust coefficient indicates that nozzle "B" was the most efficient nozzle (the higher the better). Also, the difference between the divergent section, related to average thrust, does not shown significant changes for the measured pressure range. Once was expected that the nozzles with divergent sections would have better global efficiency parameters compared with nozzles without this type of section.
- The equation for KNSu burn rate with the absolute pressure is: $r = 0,012 p_0^{0,475}$
- The equation for KNSu burn rate with the estimated pressure is: $r = 0,018 p_0^{0,440}$
- Additional investigation related to combustion instability for the KNSu propellant is strongly suggested.
- Is noticeable that some considerable variability exist between each IBR test in Fig. 13 and Fig. 14. Probably, this was motivated due to nozzles throat diameter variations and its low combustion pressure. Additional static tests are recommended for reinforce the results found by this work. More details can be found in Américo (2018).

8. ACKNOWLEDGEMENTS

The authors would like to acknowledge the financial support provided by CNPq, since the third author is supported by a CNPq scholarship, and CAPES, both Brazilian agencies for the fostering of sciences, and also, Positivo University, because this article were written based on first author undergraduate research Américo (2018), to obtain his Bachelor Degree in Mechanical Engineering.

9. REFERENCES

Américo, C.E., 2018. *Desenvolvimento de um motor-foguete de teste balístico.* Graduação em Engenharia Mecânica, Universidade Positivo.

Foltran, A.C., Moro, D.F., da Silva, N.D.P., Ferreira, A.E.G., Araki, L.K. and H., M.C., 2014. "Medição da velocidade de queima a pressão atmosférica do propelente sacarose/nitrato de potássio preparado a frio." *Simpósio Aeroespacial Brasileiro.*

Germer, E.M., 2014. *Avaliação do efeito da geometria da seção convergente em tubeiras de motor-foguete.* Doutorado em Engenharia Mecânica, Universidade Federal do Paraná.

GFCS, 2018. "Curva empuxo 3p2". http://servidor.demec.ufpr.br/foguete/Aplicativos/. Accessed in: 08/07/2018.

Humble, R.W., Henry, G.N. and Larson, W.J., 1995. *Space Propulsion Analysis and Design*. McGraw Hill.

Miller, W.H., 1971. "Solid rocket motor performance analysis and prediction". *Monograph - National Aeronautics and Space Administration*.

Nakka, R., 1999. *Effect of chamber pressure on burning rate for the Potassium Nitrate - Dextrose and Potassium Nitrate - Sorbitol rocket propellants*.

Nakka, R., 2001a. "Burn rate determination from a pressure-time trace." http://nakka-rocketry.net/ptburn.html. Accessed in: 08/07/2018.

Nakka, R., 2001b. "Amateur experimental solid propellants." http://nakka-rocketry.net/propel.html. Accessed in: 08/07/2018.

Nakka, R., 2003. "Solid propellant burn rate." http://nakka-rocketry.net/burnrate.html. Accessed in: 08/07/2018.

OSP, 2018. "Tracker - video analysis and modeling tool". https://www.physlets.org/tracker/. Accessed in: 08/07/2018.

Sutton, G.P. and Biblarz, O., 2008. *Rocket Propulsion Elements*. John Wiley & Sons.

10. RESPONSIBILITY NOTICE

The authors are solely responsible for the printed material included in this paper.